RESEARCH *New Phytol.* (2000), **146**, 235–247

Changes in axial hydraulic conductivity along elongating leaf blades in relation to xylem maturation in tall fescue

PIERRE MARTRE[1], JEAN-LOUIS DURAND[1]* AND HERVE COCHARD[2]

[1] *Unité d'Ecophysiologie des Plantes Fourragères, Institut National de la Recherche Agronomique, F-86 600 Lusignan, France*
[2] *Unité de Physiologie Intégrée des Arbres Fruitiers, Institut National de la Recherche Agronomique, F-63 039 Clermont-Ferrand, France*

Received 26 July 1999; accepted 5 January 2000

SUMMARY

Xylem maturation in elongating leaf blades of tall fescue (*Festuca arundinacea*) was studied using staining and microcasting. Three distinctive regions were identified in the blade: (1) a basal region, in which elongation was occurring and protoxylem (PX) vessels were functioning throughout; (2) a maturation region, in which elongation had stopped and narrow (NMX) and large (LMX) metaxylem vessels were beginning to function; (3) a distal, mature region in which most of the longitudinal water movements occurred in the LMX. The axial hydraulic conductivity (K_h) was measured in leaf sections from all these regions and compared with the theoretical axial hydraulic conductivity (K_t) computed from the diameter of individual inner vessels. K_t was proportional to K_h throughout the leaf, but K_t was about three times K_h. The changes in K_h and K_t along the leaf reflected the different stages of xylem maturation. In the basal 60 mm region, K_h was about 0.30 ± 0.07 mmol s^{-1} mm MPa^{-1}. Beyond that region, K_h rapidly increased with metaxylem element maturation to a maximum value of 5.0 ± 0.3 mmol s^{-1} mm MPa^{-1}, 105 mm from the leaf base. It then decreased to 3.5 ± 0.2 mmol s^{-1} mm MPa^{-1} near the leaf tip. The basal expanding region was observed to restrict longitudinal water movement. There was a close relationship between the water deposition rate in the elongation zone and the sum of the perimeters of PX vessels. The implications of this longitudinal vasculature on the partitioning of water between growth and transpiration is discussed.

Key words: elongating leaf (elongation zone), hydraulic conductivity (xylem conductivity, radial conductivity), protoxylem-metaxylem transition, tall fescue (*Festuca arundinacea*), water transport, xylem maturation, xylem microcasting.

INTRODUCTION

In grasses, growth occurs at the base of the expanding leaves. Areas of undifferentiated and maturing cells (growth zone) are therefore found between fully functional tissues, located below in the stem and above in the mature part of the leaf. This structure raises many questions about the efficiency of water transfer within growing leaves. Indeed, water flow in an elongating leaf is important for two reasons. First, a small amount of water must flow from the roots to the growth zone itself to sustain tissue expansion. The spatial arrangement and surface area as well as the properties of the cell wall of the protoxylem (PX) hence play a role in the growth-related radial water flow. Second, once the growing leaf emerges from the whorl of the older leaf, a more substantial amount of water needs to flow through the growth zone to compensate for water losses by transpiration. That situation lasts for half the duration of leaf elongation (Durand *et al.*, 1999). There is evidence from the literature that the

Abbreviations: d_{water}, local net water deposition rate (mmol s^{-1} mm^{-1}); K_h, measured axial hydraulic conductivity of the xylem (mmol s^{-1} mm MPa^{-1}); k_t, theoretical axial hydraulic conductivity of an individual vessel (mmol s^{-1} mm MPa^{-1}); K_t, theoretical axial hydraulic conductivity of all functioning vessels in parallel (mmol s^{-1} mm MPa^{-1}); K_t*, theoretical axial hydraulic conductivity of all functioning vessels (in parallel), corrected on the basis of the K_h:K_t ratio (mmol s^{-1} mm MPa^{-1}); Lp_{px}, radial hydraulic conductance of vessel cell wall for water flow from the protoxylem in the elongation zone to the surrounding expanding mesophyll (mmol s^{-1} mm^{-2} MPa^{-1}); LMX, large metaxylem; MX, metaxylem; NMX, narrow metaxylem; REGR, relative elemental growth rate (h^{-1}); PX, protoxylem.

*Author for correspondence (fax +33 5 49556068; e-mail: jldurand@lusignan.inra.fr).

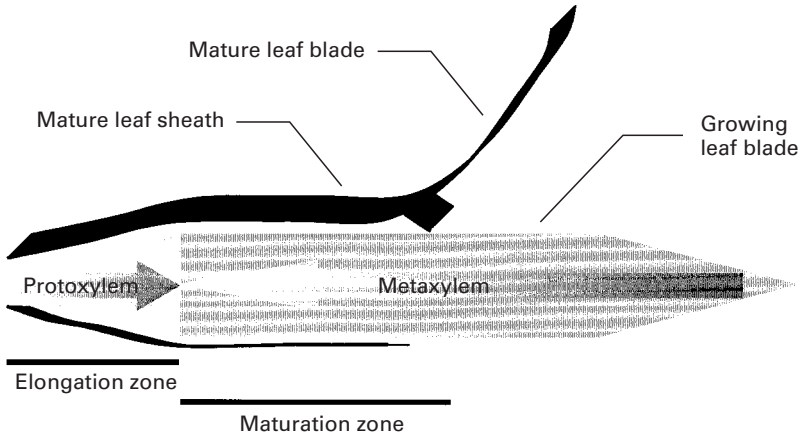

Fig. 1. Diagrammatic representation of the dynamics of xylem maturation within a growing grass leaf. Protoxylem (PX) maturates acropetally in the basal elongating region of the leaf blade. Metaxylem (MX) matures basipetally in the maturation zone of the blade.

leaf elongation rate might decline within seconds in response to atmospheric or edaphic water deficits (Frensch, 1997). Cells in the growth zone have significantly lower water potential values than expanded cells of the maturation zone (Matsuda & Riazi, 1981; Michelena & Boyer, 1982; Barlow, 1986; Fricke & Flowers, 1998; Martre *et al*., 1999). A water potential difference between the water source (xylem) and sink (expanding mesophyll cells) is a prerequisite for growth. A reduction in water availability or an increase in transpiration might then induce an immediate reduction in the water potential difference and impair cell growth (Westgate & Boyer, 1984). In order to understand the causal relationships between leaf growth and leaf water supply, it is necessary to understand the mechanism and structure of the water-transfer efficiency within a growing leaf.

The vascular arrangement of the elongating grass leaf was documented some time ago (Esau, 1965). First to differentiate are PX vessels; they are usually mature (i.e. able to conduct sap) before the leaf undergoes intensive elongation. New PX vessels continue to differentiate and mature in the growth zone (Fig. 1). Metaxylem vessels which appear after the PX differentiate in the growth zone, but in contrast with the PX, mature only beyond the elongation zone (i.e. once they have stopped elongating). Although the anatomy of the elongating grass leaf is known, the real function of its different xylem vessels and water-transport capacity remains unclear. Within the growth zone, xylem vessels have to be sufficiently longitudinally extensible to increase in length, but also sufficiently radially rigid to hold water columns under tension. Because PX elements mature within the growth zone, they can be stretched so much that their modified primary walls can be disrupted, which might eventually impair their function, and the PX could be replaced by a lacuna. Are the protoxylem lacunae immediately replaced by new xylem vessels or is the growth zone devoid of intact conducting elements for a given period? Recently, Evert *et al*., (1996) and Trivett & Evert (1998) in studies of maize and barley leaves, respectively, supported the conclusion of Sharman (1942): 'the protoxylem collapses completely during the last extension of the surrounding tissues and before the basipetally differentiating metaxylem elements reach maturity in that region. Hence, until mature xylem elements are present there, the distal portion of the leaf would have no direct connection with the stem by means of differentiated tracheary elements'. However, Rayan & Matsuda (1988) have shown that in young barley leaves functional vessels extend from the intercalary meristem to the mature part of the elongating blade and that water moves through the growth zone in vessels and not intercellularly. Similarly, in the first leaf of the wheat seedling, Paolillo (1995) has shown that the dynamics of vessel maturation and vessel collapse allow the xylem as a whole to remain functional across the growth zone. The fully elongated metaxylem (MX) vessels develop basipetally above the elongation zone and spatially overlap the PX elements, which should ensure vascular continuity throughout the leaf.

However, no measurement of axial hydraulic conductivity of the xylem (K_h) has ever been made in these regions of the leaf. The objective of our study was to assess the changes in xylem functionality along the elongating leaf of tall fescue (*Festuca arundinacea*). The hypothesis of xylem continuity throughout the immature part of the blade was tested. Unlike previous studies, our analysis was both qualitative and quantitative. The patterns of xylem maturation and the spatial overlap of PX vessels with MX vessels were described. To determine whether a vessel was cytoplasm-free and actually conducted water, both staining and microcasting were performed. Xylem vessel diameter was measured at different levels of the growing leaf in order to compute a theoretical axial hydraulic conductivity (K_t*) along the growing lamina.

Finally, the axial hydraulic conductivity (K_h) was measured in leaf sections to validate the computation of K_t* and to determine whether the elongation zone restricts hydraulic conductivity, producing a bottleneck in longitudinal water transport.

MATERIAL AND METHODS

Plant material and growth conditions

All experiments where carried out using the same clone of tall fescue (*Festuca arundinacea* Schreb. cv. Clarine). A single parent plant was vegetatively propagated in a controlled-environment cabinet. Tillers were separated, roots removed, shoots cut into 70-mm-long stubbles, and the tiller bases were placed in sand for 21 d. Rooted tillers were then transferred to hydroponic culture on the solution described by Maurice *et al*. (1997). Tillers were harvested from days 14–21 after the plants were transferred to hydroponic solution when the third uncut leaf (L_3) was 200 ± 10 mm long (i.e. approx. 50% of final length). At this stage, the ligule of L_3 was <1 mm from the leaf base. L_3 was the last leaf to emerge from the enclosing older leaf sheath. The leaves which were one and two plastochrons older are referred to as L_2 and L_1 respectively. To further homogenize the leaf population, only tillers whose L_1 sheath lengths were similar (100 ± 5 mm) were selected.

Conditions in the controlled-environment cabinet were the same throughout the experiment. The PPFD was 530 ± 10 μmol m^{-2} s^{-1} (provided by an HQI-400 W/D lamp, Osram, München, Germany) during the 14 h of photoperiod. Relative humidity was controlled at 85 ± 2% throughout the 24-h period, and air temperature was set at 18/24°C (light/dark) in order to ensure a constant temperature (24 ± 0.5°C) in the leaf elongation zone (Durand *et al*., 1999).

Relative elemental growth rate

The relative elemental growth rate (REGR) was determined by the pricking method described by Schnyder *et al*. (1987): holes were pricked every 5 mm through the 60-mm-long basal part of the tiller with a fine entomologist's needle (0.2 mm diameter). Pricking was performed at 4 h and sampling at 10 h into the 10-h dark period. The elongation of L_3 between pricking and sampling was 8–15% of the length of the elongation zone. REGR at any distance x from the leaf base ($r(x)$, h^{-1}) was calculated as:

$$r(x) = \frac{\delta(x)}{l(x)\Sigma\delta(x)}\, v_{max} \qquad \text{Eqn 1}$$

(x is the distance from the line of attachment of the leaf to the node, $\delta(x)$ is the elongation of a segment delimited by two neighbouring pinholes and whose midpoint is initially at x, $l(x)$ is the initial length (mm) of the section at initial position x, and v_{max} is the leaf elongation rate.) To calculate v_{max}, the distance between the tip of L_3 and the ligule of L_1 was measured at the pricking and sampling times on matched unpricked leaves (Schnyder *et al*., 1987).

Net water deposition rate

At the end of the dark period, nine tillers were sampled. L_3 was removed from each of the surrounding sheaths in a humid saturated box, and starting from the leaf base (i.e. at the point of insertion on the stem), 10 5-mm-long sections were sampled. After fresh weight was determined, the sections were dried at 70°C for 48 h and dry weight was measured. The water content (r, mmol mm^{-1}) of samples was calculated as the difference between fresh and dry weight per unit of tissue length.

The local net rate of water deposition (d_{water}), mmol of water per s and per mm of tissue) along the elongation zone was calculated using the one-dimensional version of the continuity equation described by Silk (1984):

$$d_{water}(x) = \frac{\delta\rho(x)}{\delta t} + \upsilon(x) \times \frac{\delta\rho(x)}{\delta x} + \rho(x) \times r(x) \qquad \text{Eqn 2}$$

(t is the time (s) and $\upsilon(x)$ is the displacement velocity at position x (mm s^{-1}).) Schnyder & Nelson (1988) have shown that during the night period the spatial distribution of water content within the elongation zone was relatively steady. Therefore, the local rate of change $\delta\rho(x)/\delta t$) was neglected.

The gradient of water content $\delta\rho(x)/\delta x$) was calculated as described by Schnyder & Nelson (1987):

$$\frac{\delta\rho(x)}{\delta x} = 0.5 \times \left[\left(\frac{\rho_i - \rho_{i-1}}{x_i - x_{i-1}}\right) + \left(\frac{\rho_{i+1} - \rho_i}{x_{i+1} - x_i}\right)\right] \qquad \text{Eqn 3}$$

(ρ_i is the water content in section i, and x_i is the position of the midpoint of section i.) For the first section from the base, $\delta\rho(x)/\delta x$ was calculated as $(\rho_{i+1} - \rho_i) \times (x_{i+1} - x_i)^{-1}$.

Staining

To assess which vessels carried water through the elongating leaf, the leaf was perfused with a dye, an acid solution of alcian blue, used because it flowed rapidly into vessels and diffused slowly out of their lumina, allowing testing of the function of individual vessels in a bundle. Ten tillers were cut under water at the root–shoot junction and tightly fitted into a tube filled with a 0.1% (w/v) alcian blue solution in 10 mM citric acid, filtered to 0.45 μm. The dye solution was injected under a 20 kPa hydrostatic pressure gradient for 2 h. This duration was

determined after many preliminary assays of 20 min–24 h under varying pressure (5–20 kPa) and was chosen because it coloured all functional vessels without lateral diffusion of the dye. In order to show whether some metaxylem vessels which mature basipetally were functional although they did not carry water in the normal direction of water flow, staining was also performed from the distal part of the blade. Freehand cross sections were then taken every 10 mm from the base to the tip of the leaf and observed under an Olympus BH2 microscope (Olympus, Lake Success, NY, USA) at a magnification of 400x. The numbers of unstained and stained vessels were counted. In each cross section, all the vessels (PX, NMX and LMX) were considered.

Xylem microcasting

Xylem microcasting was performed according to the technique of André (1993): growing leaves (nine samples) were dehydrated by successive immersion in 50% acetone/ethanol solution (v/v) at 60°C for 2 h and absolute ethanol at 60°C for 10 min. Leaves were then cut with a fresh razor blade into 20-mm sections, and placed in a vacuum for a few minutes to evaporate any liquid in the vessels. They were then immersed in fluid silicon elastomer (RTV 141, Rhône-Poulenc, Saint Fons, France) under a vacuum of 7 kPa for 2 h. When atmospheric pressure was restored, the elastomer filled all the apoplastic space in the leaf. Leaf sections in the elastomer were maintained at −18°C for 12 h to avoid reticulation of the elastomer during the filling of the vessels. The elastomer was stopped by an intact pit membrane, but easily passed through the perforations.

The elastomer was reticulated at 40°C for 4 h. Cell walls and biological material where then destroyed by successive immersion in concentrated solutions of sulphuric acid (24 M), sodium bicarbonate (1.3 M) and sodium hypochlorite (2 M). The cast samples were carefully dissected under a binocular microscope to show the vascular arrangement, and cast vessels were separated from each other on a water film. Some vessel casts were removed and observed with a scanning electron microscope (model JSM-35CF, Jeol Corp., Tokyo, Japan) at 15 kV after standard gold coating.

Hydraulic conductivity

Under water, 20 growing L_3 leaves were separated from the rest of the tiller and cut into 40-mm-long sections. They were wrapped longitudinally around a 20-mm-long aluminium bar of 4 or 1.5 mm diameter, depending on leaf width, covered with Teroson in order to prevent leaks at the furrows of the leaf. Leaf sections around the bar were covered with Teflon tape and *c*. 5 mm was cut off each end with a fresh razor blade immediately before fitting both ends into an apparatus adapted from Sperry *et al*. (1988). The apparatus was configured to accommodate six samples. The axial hydraulic conductivity (K_h, mmol s^{-1} m MPa^{-1}) was defined as the fluid flux rate (mmol s^{-1}) divided by the pressure gradient (MPa mm^{-1}) along the section. The pressure gradient was induced by a hydrostatic pressure head of 6 kPa. Deionized, degassed 0.1% (v/v) concentrated HCl (37.7%) solution (*c*. pH 2) filtered to 0.2 μm flowed through plastic tubing connecting the end of the section to a reservoir postioned on an analytic balance (model R180D, 10^{-5} g resolution) (Sartorius Corp., Bohemia, NY, USA) enabling measurement of water flow. Weight was monitored every 30 s by a microcomputer through a serial communication interface. After measurement of K_h, length, thickness and width of the leaf sections were measured with a calliper rule (10 μm resolution). Using an alcian blue solution, we checked that water flowed only in the vessels and not in the intercellular spaces during these measurements.

In sections taken >30 mm from the leaf base, one freehand cross section was cut from the middle of the sections immediately after measurement of K_h. The more basal sections were impossible to remove from the bar without damage. Autofluorescent xylem vessels were measured, since blue fluorescence of the cell wall is indicative of wall lignification (linkage of ferulic acid and lignin (Fukazawa & Imagawa, 1981)).

The sections were viewed with a fluorescence microscope (model BH2-RFC, Olympus) fitted with a 20UG1 exciter filter (excitation wavelength of 334–365 nm), a DM 400 dichromatic mirror and a 17L420 barrier filter (barrier wavelength minimum = 420 nm) and a magnification of 400x. The inner diameter of individual xylem vessels was measured with a tube-mounted light chamber and a digitizing board (Model 23120, CalComp, Anaheim, CA, USA) with a resolution of 0.1 μm. The vessels were considered elliptical in cross section, and the length of the two axes was measured.

The theoretical axial hydraulic conductivity of individual xylem vessels (k_t) was calculated according to the Poiseuille equation for elliptical vessels (Lewis & Boose, 1995):

$$k_t = \frac{\pi}{64\eta} \frac{a^3 b^3}{a^2 + b^2} \qquad \text{Eqn 4}$$

(η is the viscosity of water (MPa s^{-1}), and a and b are the short and the long axes (μm) respectively.)

Thirty-millimetre-long sections were used to measure K_h. Since the transition zone between the PX and LMX extended over only a few centimetres, the spatial pattern of longitudinal vasculature was described more accurately by measuring the number and diameter of xylem vessels in cross section taken

from a second batch of eight tillers. Tillers were excised at the root–shoot junction, the first cut leaves were removed, then cut again into 50-mm sections and fixed for 30 min under a vacuum in 2% paraformaldehyde (v/v), 1% glutaraldehyde (v/v) and 1% caffeine (w/v) solution in a 0.2 M phosphate buffer at pH 7.2. Following fixation, freehand cross sections of L_3 were cut with a razor blade every 5 mm for the part of the leaf still enclosed in the sheath of L_1, and every 10 mm for the emerged part. Sections were mounted in 20% glycerol between a slide and a cover slide. The number of bundles and the number of PX and LMX fluorescent vessels in each bundle were counted and the lengths of the two axes of individual vessel lumina were measured under a fluorescence microscope as described above. The diameter of individual vessel lumina was calculated as the diameter of a circle of equivalent perimeter

$$D = \frac{\overline{a^2+b^2}}{2} \qquad \text{Eqn 5}$$

(k_t for each vessel was computed using Eqn 4.)

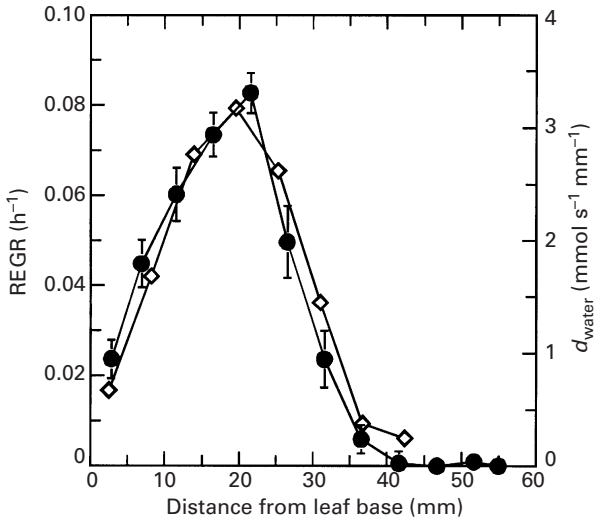

Fig. 2. Spatial distribution of the relative elemental growth rate (REGR, circles) and of the local net water deposition rate during the dark period (d_{water}, diamonds) in the elongation zone of tall fescue leaf blades, during the dark period. Data are means ± SE (represented by vertical bars, except when smaller than the symbol), $n = 9$.

RESULTS

Growth

At the developmental stage at which the tillers were sampled, two elongating leaves (L_2 and L_3) were visible. The youngest expanding leaf (L_4) was totally enclosed and was about 20 mm long. In this work, only L_3 is considered. At this stage, daily increase in L_3 length was almost constant for 4 d (data not shown), averaging 1.3 ± 0.05 mm h^{-1} ($n = 31$). The length of the elongation zone was 38 ± 2 mm (Fig. 2).

The REGR was at a maximum (0.83 ± 0.04 h^{-1}) 21 mm from the leaf base (i.e. in the middle of the elongation zone) (Fig. 2). These results were in agreement with data from Durand *et al.* (1995), Maurice *et al.* (1997) and Martre *et al.* (1999) on tall fescue. The spatial distribution of d_{water} closely followed that of the REGR, reaching a maximum 21 mm from the base. It almost reached zero at the end of the elongation zone (i.e. 38 mm from the leaf base), indicating that volume growth was almost restricted to the elongation zone.

Xylem organization

Three classes of longitudinal bundles were defined following the Ellis classification (1976): large (containing PX, LMX and NMX vessels), intermediate (containing LMX and NMX vessels) and small (containing only NMX vessels). At any level of L_3, all large bundles had at least one fluorescent vessel. The number of large bundles decreased along the leaf from 9.8 ± 0.1 5 mm from the base to 2.5 ± 0.2 20 mm from the tip (Fig. 3a). The first small bundle containing at least one lignified (fluorescent) xylem vessel appeared at 65 mm from the base, indicating a basipetal differentiation. Beyond 65 mm, the number of small bundles increased to 12.8 ± 0.6 in 20 mm, and remained almost constant beyond 85 mm. The pattern of bundles was regular, large bundles alternating with small ones. At that developmental stage, there was no intermediate bundle in L_3.

The number of PX vessels was at a maximum (20.7 ± 1.2) approximately 20 mm from the leaf base (i.e. at the middle of the elongation zone) (Fig. 3b). Beyond that, it decreased down to the tip of the leaf (2.3 ± 0.9). In the elongation zone, there was no fluorescent metaxylem vessel. The first fluorescent LMX vessel was found 35 mm from the base, but it was not mature at that position, as the thickness of its cell wall increased at least up to 45 mm (data not shown). Beyond 35 mm, the number of fluorescent LMX vessels increased rapidly, and beyond 80 mm from the base the number of LMX vessels was almost constant and close to 27 ± 0.6. Fluorescent NMX were found at 85 ± 10 mm from the base in small bundles and at 60 ± 10 mm from the base in large bundles (data not shown).

The mean diameter of PX vessels was at a maximum (16.5 ± 0.5 μm) 20 mm from the leaf base (i.e. at the middle of the elongation zone) (Fig. 3c). Beyond that, it decreased to 10.1 ± 0.2 μm near the leaf tip. This indicated that at this developmental stage of L_3, the PX diameter was probably still increasing. The mean diameter of LMX vessels was close to 31 μm 40–70 mm from the leaf base, then decreased to 23.8 ± 0.6 μm near the leaf tip. The mean diameter of NMX vessels remained unchanged along the leaf and was equal to 5 ± 0.2 μm (data not

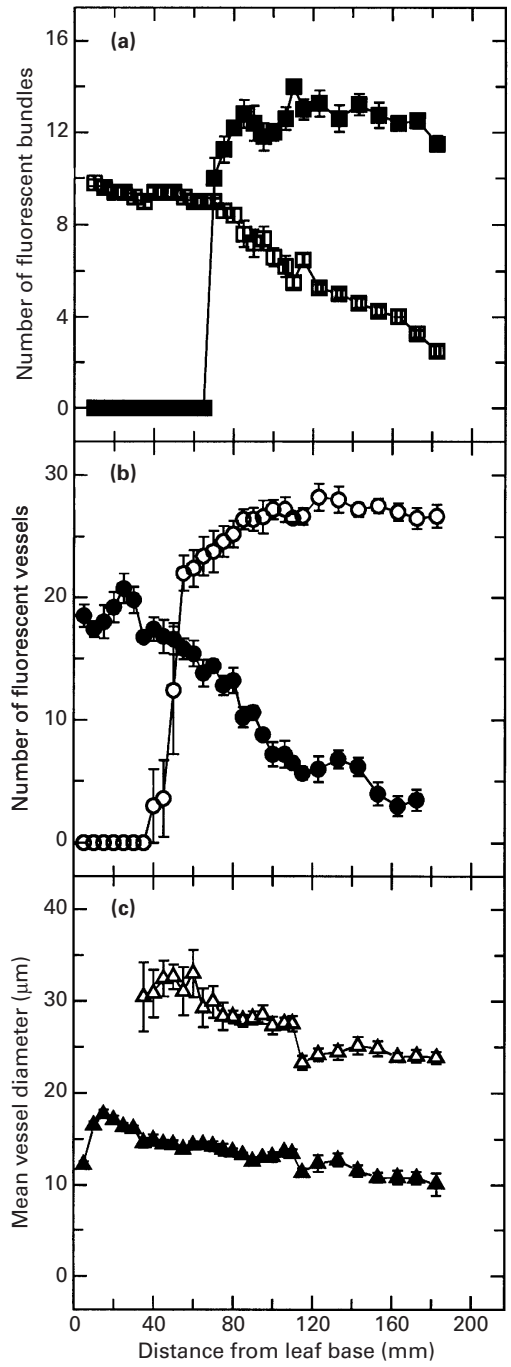

Fig. 3. Number of small (filled squares) and large (open squares) bundles containing at least one autofluorescent vessel (a), number of PX (filled circles) and LMX (large metaxylem, open circles) autofluorescent vessels (b), mean diameter of PX (filled triangles) and LMX (open triangles) auto-fluorescent vessels (c), in relation to their positions along elongating leaf blades of tall fescue. Data are means ± SE, $n = 8$.

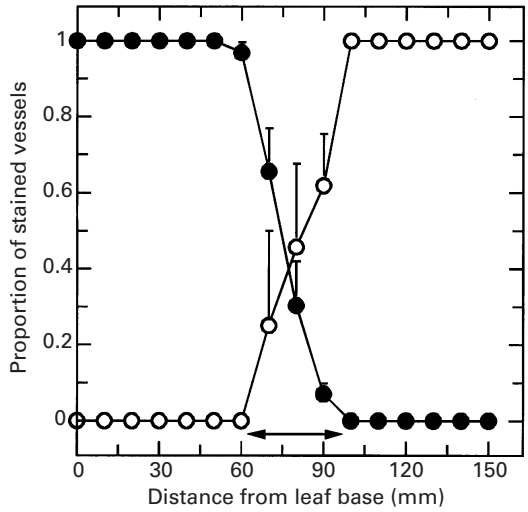

Fig. 4. Proportion of stained PX (filled circles) and LMX vessels (open circles) in relation to their position along elongating leaf blades of tall fescue. Vessels were coloured from the basal or the distal end of the leaves by a solution of alcian blue. Dye flow was induced by a hydrostatic pressure gradient of 20 kPa for 2 h. Data are means + SE, $n = 10$. The horizontal arrow indicates the region where narrow metaxylem (NMX) vessels were stained. It also corresponds to the transition zone of the water flux from PX to LMX vessels.

shown). Because of their small diameter, NMX vessels contributed only $3 \pm 1\%$ ($n = 13$) of the conductivity in the leaf section and were not systematically measured.

To determine which vessels were functional along the elongating leaf blade, a solution of alcian blue was flushed from the leaf base to the tip. The proportion of PX and LMX stained vessels in the large bundles changed according to their position along the leaf blade (Fig. 4). From the base–60 mm, all PX vessels in all large bundles were stained. This proportion rapidly decreased to zero at approximately 100 mm from the base. From the base–60 mm, no LMX vessel was stained. Almost symmetrically, the proportion of stained LMX vessels rapidly increased up to one at approximately 100 mm from the base, indicating that the alcian blue solution had passed from PX to LMX vessels within a zone of approximately 40 mm, starting at 60 mm from the leaf base. This showed that either PX vessels were disrupted beyond 60 mm, or that they were so narrow that the water flux in the PX was very low compared with that in the LMX. Although the proportion of stained NMX vessels could not be measured with the same accuracy as that of LMX and PX, stained NMX could only be viewed in the region 60–110 mm from the base, reaching a maximum at *c.* 90 mm from the leaf base.

When the dye was perfused basipetally from the cut tip of the leaf in large bundles, the same results were obtained as in the acropetal direction. In small bundles, as NMX vessels maturated basipetally all NMX were coloured from the tip to 120 mm from the base, but beyond that, the number of coloured NMX decreased rapidly, and 70 mm from the base none could be observed (data not shown) (Fig. 5).

In order to determine more accurately the location and spatial arrangement of the transition zone between PX and LMX vessels, 20-mm-long sections

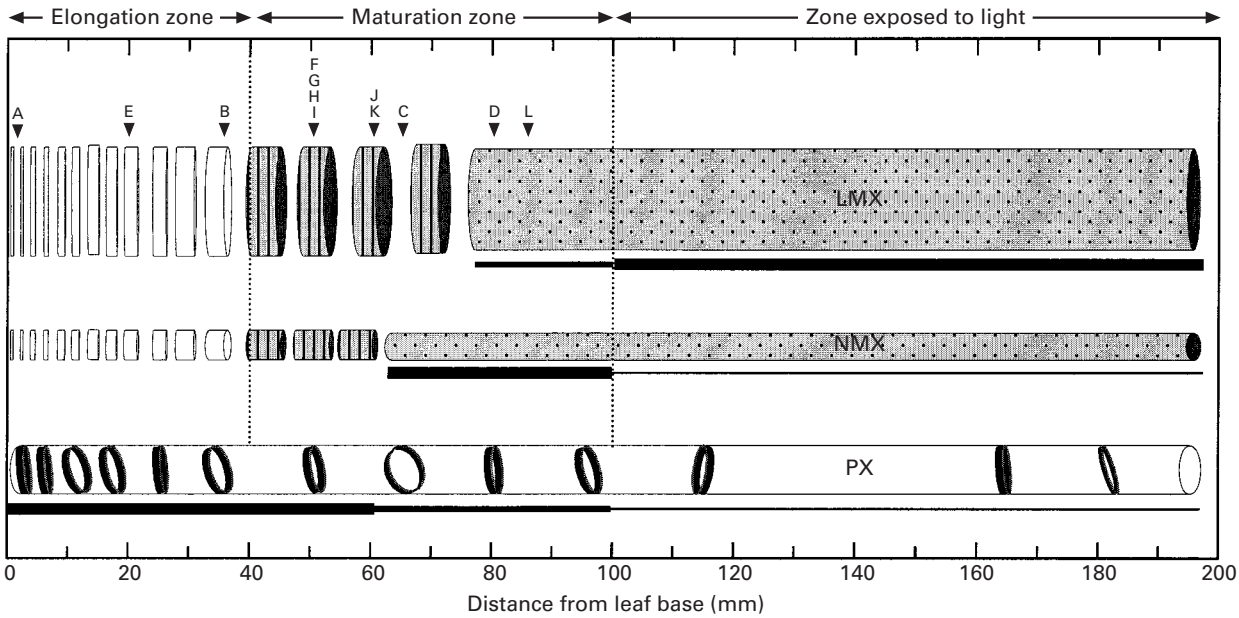

Fig. 5. Diagram of xylem maturation in large bundles of elongating tall fescue leaves. (a–l) Locations of Fig. 6 micrographs. White discontinuous area in NMX and LMX, unlignified expanding vessel elements. Hatched discontinuous area of NMX and LMX in maturation zone, expanded vessel elements, where secondary wall formation is under way. Lines under each vessel, function of each vessel type in terms of water conductance; thickness of lines indicates relative contribution (nonscaled) to water flux. Vessels are proportionally scaled in length and width. Small bundles present the same profile of xylem maturation, but consist solely of NMX vessels.

of L_3 vessels were cast (Fig. 6a–n; see Fig. 5 for spatial localization of micrographs). Intact cast PX vessels were found in all leaf sections, indicating that the PX was continuous throughout the leaf. PX underwent extensive stretching (approx. 10-fold) without rupturing when passing through the elongation zone (Fig. 6a–b). When the primary modified cell wall of PX vessels had been so severely stretched that it tore, the elastomer invaded the intercellular space between vessel elements (e.g. vessel 1 in Fig. 6i). Consistent with previous results (Figs 3, 4), the first cast metaxylem elements appeared 60–70 mm from the leaf base (Fig. 6c). Their diameter was small (NMX), and less than that of PX vessels. In cross section, they corresponded to the vessels located between the PX and LMX vessels (Fig. 6o). The first NMX vessels were adjacent to PX vessels, their dense pitted walls and the primary cell walls of PX vessels faced each other (Fig. 6j–k). NMX vessels exhibited a continuous basipetal differentiation. Their number rapidly increased, and at 80–100 mm the first LMX appeared (Fig. 6d). The diameter of LMX vessel elements was *c.* five times greater than that of NMX elements (Fig. 6l). The perforation plates were visible in the transparent elastomer under light microscopy. Both LMX and NMX vessel elements had simple perforation plates, surrounded by a punctuation field (Fig. 6 m).

In some bundles, the last mature protoxylem vessels exhibited a different ornamentation in and above the elongation zone. In one case (Fig. 6f–h) this ornamentation changed within a range of a few μm from annular to reticulate, but in other cases we observed a 10–400-μm-long intermediate scalariform or reticulate pattern.

Axial hydraulic conductivity

K_h of L_3, measured in 30-mm leaf sections, increased from 0.3 ± 0.07 mmol s^{-1} mm MPa^{-1} 19 mm from the leaf base to 5.0 ± 0.31 mmol s^{-1} mm MPa^{-1} 105 mm from the base. K_h then decreased to 3.5 ± 0.21 mmol s^{-1} mm MPa^{-1} at the leaf tip (Fig. 7).

Measured conductivity values of sections > 60 mm from the leaf base were compared with K_t, which was computed from k_t calculations (eqn 4) and the proportions of functional PX and LMX:

$$K_t(x) = \alpha_{PX}(x)\Sigma k_{tPX}(x) + \alpha_{LMX}(x)\Sigma k_{LMX}(x) \quad \text{Eqn 6}$$

($\alpha_{PX}(x)$ and $\alpha_{LMX}(x)$ are the proportions of functional PX and LMX vessels, respectively, at position x, and $\Sigma k_{tPX}(x)$ and $\Sigma k_{tLMX}(x)$ are the sums of the conductivity of individual PX and LMX vessels, respectively, at position x.) Following the results of staining and microcasting, α_{PX} was set to one, assuming that all PX vessels remained functional throughout the leaf, and that α_{LMX} was equal to the observed proportion of coloured LMX (Fig. 4). K_h was linearly correlated with K_t, with $r = 0.86$, $P < 0.05$ (Fig. 8), but K_h was only $36 \pm 4.5\%$ of K_t (Fig. 8).

For the other batch of 8 tillers, where xylem vessels were measured with higher spatial resolution (Fig. 4), K_t was corrected (K_t*) by an impediment

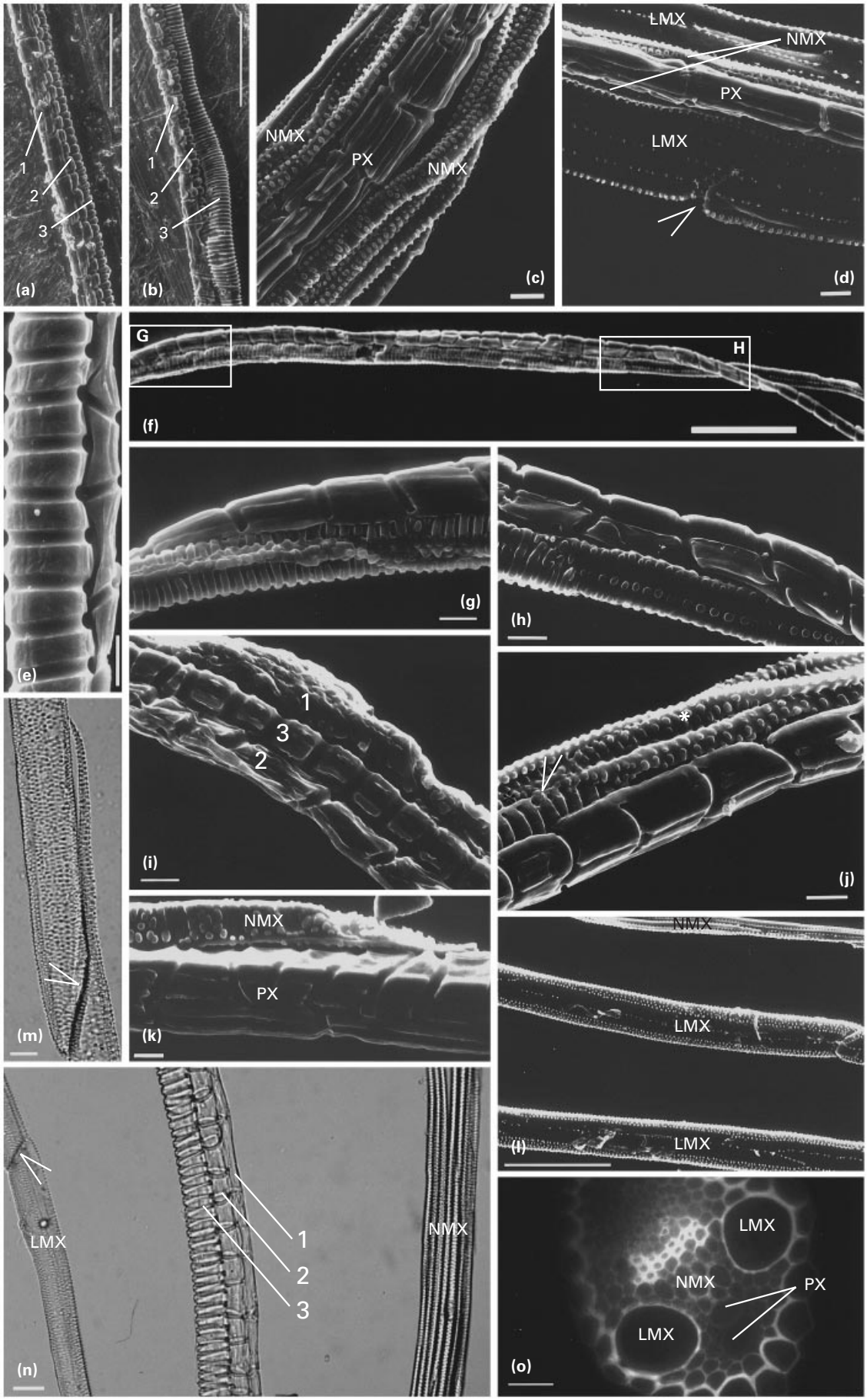

Fig. 6. For legend see opposite.

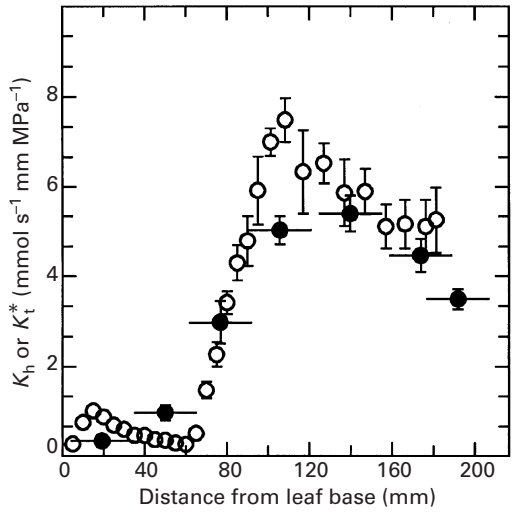

Fig. 7. Measured axial hydraulic conductivity of the xylem (K_h, filled circles) and corrected theoretical axial hydraulic conductivity (K_t*, open circles) in relation to their position along elongating leaf blades of tall fescue. K_h was measured on 30-mm sections; horizontal bars represent the length of the section. See text for details of K_t* computation. Data are means ± SE (represented by vertical bars, except when smaller than the symbol), n = 12–20 (K_h) and 8 (K_t*).

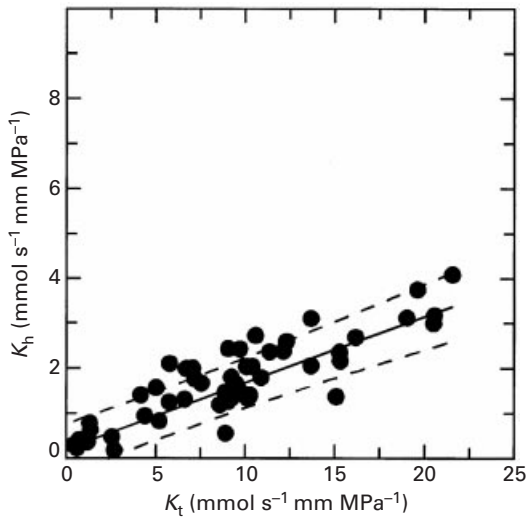

Fig. 8. The relationship between theoretical (K_t, predicted from Poiseuille equation for ideal capillaries) and measured (K_h) axial hydraulic conductivity of 30-mm sections of tall fescue elongating leaf blades. Each point represents a single section taken from 30–170 mm from the base. K_t was computed from individual metaxylem diameter measurements, in cross sections taken from the middle of the section where K_h was previously measured. All fluorescent PX and LMX vessels in a cross section were measured. Straight line, linear regression (y = 0.36x + 0.04, r = 0.86, P<0.05); dashed lines, 95% confidence intervals.

coefficient, C, defined as a correction factor by which K_t had to be multiplied in order to give the measured value of axial hydraulic conductivity (K_h). C was determined to be equal to 0.36 (Fig. 8). We made the assumption that C was the same for proto- and metaxylem vessels. K_t* varied within the same range as K_h (i.e. 1–7 mmol s^{-1} mm MPa^{-1}. The general pattern of variation of K_t* (Fig. 7) was similar to that of K_h, with the same large difference between the basal and the apical region of the leaf. The largest discrepancy between K_h and K_t* was *c.* 110 mm from the base, where the expected K_t* exceeded K_h by about 30%.

In the elongation zone, K_t* exhibited a local maximum roughly at the middle of the elongation zone. This pattern of K_t* was due to the variation in

Fig. 6. (a–l) Scanning electron micrographs of vascular bundles cast in rapidly elongating leaf blades of tall fescue. (a) PX vessels isolated from a large bundle 2 mm from the base in the division zone and numbered in order of maturation. PX 1 was extremely stretched and discontinuous, whereas the PX 3 vessel wall had not yet been stretched. PX 2 was intermediate in the developmental stage (bar, 100 μm). (b) PX vessels isolated from the same bundle as in (a), 27 mm from the base. The rings of each vessel were more distant than in (a), but in contrast with (a), vessel 1 was not collapsed (bar, 100 μm). (c) Large bundle taken 65 mm from the base. The visible PX was partially torn, and bordered by several pitted NMX vessels (bar, 10 μm). (d) Large bundle taken at 80 mm from the base. PX and NMX vessels were flanked by two pitted LMX vessels (arrowhead, junction between the two LMX vessel elements) (bar, 10 μm). (e) Detail of two PX vessels taken 20 mm from the base (bar, 10 μm). (f) Two PX vessels taken from a large bundle 50 mm from the base; base of the leaf was on lefthand side of the micrograph. The vessel underneath had an annular ornamentation on the left and was pitted on the right (bar, 100 μm). (g) Enlargement of area G in white rectangle in (f): PX vessels with an annular wall thickening, where the vessel underneath was the last to mature (bar, 10 μm). (h) Enlargement of area H in white rectangle in (f): ornamentation of the PX vessel elements underneath changed in a few μm from an annular (left) to a pitted (right) pattern (bar, 10 μm). (i) Large bundle isolated 60 mm from the base. PX 2 and 3 were severely stretched and the primary wall was torn (bar, 10 μm). (j) Large bundle taken 60 mm from the base. Base of the leaf on lefthand side. The lower extremity of the second NMX of the bundle lay adjacent to the last mature PX vessel (arrowhead). Star, first NMX to mature (bar, 10 μm). (k) Large bundle taken 55 mm from the leaf base (right). The lower extremity of the first NMX adjacent to a PX (bar, 10 μm). (l) LMX and NMX vessels 85 mm from the base (bar, 100 μm). (m–n) Light microscopy micrographs of vascular casts. (m) Junction between two LMX vessels (arrow head: simple perforation plate) (bar, 10 μm). (n) Large bundle of mature leaf blades; arrowhead indicates simple perforation plate between two LMX vessel elements. All PX vessels were functional; vessels 1 and 2 had an annular wall thickening; vessel 3 had helical wall thickening (bar, 20 μm). (o) Hand-cut cross section of large bundle 100 mm from the leaf base, where both LMX and NMX elements were mature. PX secondary wall thickening was just under the plane of focus, and is not easily visible. Tissues that were lignified turned white because of autofluorescence under UV light (bar, 10 μm).

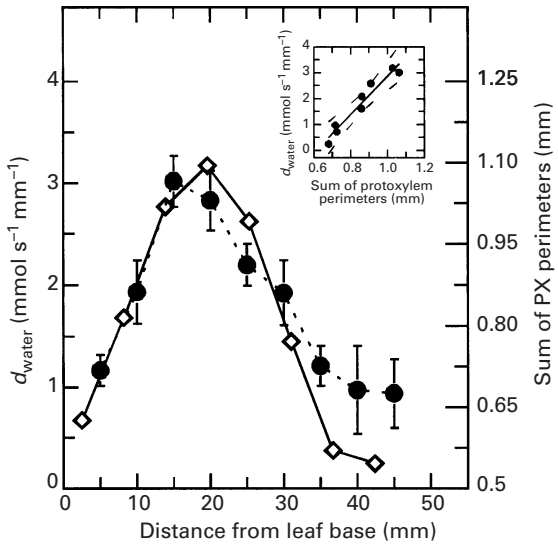

Fig. 9. The sum of PX perimeters (filled circles) in the elongation zone of tall fescue leaf blades computed from measurements of individual PX diameter in cross sections. All fluorescent PX vessels were measured. Data are means ($\pm$SE for the sum of PX perimeters), $n = 8$–9. d_{water} (open diamonds) was reported for comparison with the sum of PX perimeter. Insert, the relationship between the sum of PX perimeters and d; straight line represents linear regression ($y = 7.44x - 4.58$, $r = 0.97$, $P < 0.01$), dashed lines, 99% confidence intervals.

PX vessel number and diameter (Fig. 4), which was related to an ontological fact: older mature leaf sections have more and larger PX vessels than younger mature sections. The same pattern in the sum of the PX perimeters was observed (Fig. 9), which was closely correlated with d_{water}.

DISCUSSION

Xylem maturation and function

In elongating grass leaves, xylem hydraulic continuity from the base of the leaf to the emerged mature part was not yet clearly established. Our present results show that most of the PX vessels in each large bundle throughout the leaf remained intact. By contrast with other tissues of the leaf, vascular tissues have to differentiate and mature while they perform their function. Based on cytological observations, several published studies state that the dynamics of PX vessel replacement was not sufficient to sustain the conducting capacity of the PX until it overlapped mature metaxylem vessels (Sharman, 1942; Evert *et al.*, 1996; Trivett & Evert, 1998). In tall fescue leaf blades, the length of epidermal cells increases 10-fold as they cross the elongation zone (Durand *et al.*, 1995). In our study, PX elements underwent the same elongation (Fig. 5a–b). Despite elongation, staining showed that although PX elements appeared in cross sections to be collapsed, they still conducted the dye solution. Thus, as reported by Evert *et al.* (1985) in free-space marker studies on the maize leaf, what appeared as PX lacunae in cross sections was functioning as water-conducting conduits. Most of the stretched protoxylem vessels were not torn, since the elastomer remained in the lumina of the vessels (Fig. 5), but the cast of their primary cell walls was corrugated, reflecting the 'distortion'. We concluded that what was generally seen as a PX lacuna in cross sections was in most cases a section between two secondary wall thickenings linked by a thin, expanded (but not collapsed) primary wall. Such thin primary walls are often not seen because they are very easily dislodged by the usual methods of tissue preparation (St Aubin *et al.*, 1986). According to O'Brien (1981), the partial hydrolysis of the primary cell walls of PX facilitates the elongation of the dead PX elements by surrounding tissue. Furthermore, the bands of lignified thickening remain anchored to similar bands in neighbouring cells or to walls of lining vascular cells; this prevents the collapse of the elements undergoing stretching (O'Brien, 1981). Moreover, Ryser *et al.* (1997) have demonstrated a secretion of glycine-rich protein from the xylem parenchyma cells which is incorporated in the neighbouring primary cell wall of the PX elements. This might constitute a repair process which allows the primary wall to sustain such mechanical deformation, but as found by Dong *et al.* (1997) in older mature leaves of sugarcane, all the PX might be replaced by a lacuna which could conduct water.

As observed by MacAdam (1988) in tall fescue leaf blades, and Evert *et al.* (1996) in maize leaf blades, the distal part of the elongation zone closely corresponds to the level at which secondary wall formation is initiated in the basipetally differentiating LMX vessels. NMX vessels *c.* 20 mm below LMX vessels were mature and had an important function: to increase the exchange area between PX and LMX vessels, thereby increasing the radial hydraulic conductivity of the PX–LMX transition zone. According to the leaky pipe theory, connected elements of different diameter in a bundle constitute a functional unit (Canny, 1991). Elements of a diameter greater than a critical value ensure the axial flow, but those with a smaller diameter only allow for radial flow. Since the K_t of LMX vessels after maturation was *c.* 1000-fold ($30^4/5^4$) that of NMX vessels, beyond 100 mm from the base, axial water transport was mostly carried out by LMX. Thus, the physiological significance of the detailed sequence of tracheary element formation appears to be great.

In some bundles, the late-differentiating PX vessels, which differentiate basipetally, presented an annular or helical ornamentation in the elongation zone and a pitted ornamentation beyond this (Fig. 6g, h). These vessels were apparently transitional between the protoxylem and metaxylem (Esau, 1953). Bierhorst & Zamora (1965) and Savidge

(1996) suggested that all primary tracheary elements are constructed initially as annular or helical elements and that reticulated or pitted elements are derived ontogenetically from such elements by the addition of more wall material between the gyres of thickening. According to this hypothesis, the annular pattern of PX elements differentiated in the elongation zone might result from a duration of differentiation shorter than that of elements differentiated beyond the elongation zone. As regards the function of such transition elements, Goodwin (1942) and Paolillo & Rubin (1991) suggested that the transition from a helical or annular to a pitted pattern contributed to deceleration of elongation rate at the end of the elongation zone. It was interesting to note that functional maturity in the metaxylem was reached when or immediately before it was exposed to light, a commonly held concept in relation to grass leaves (Dale, 1985).

Axial hydraulic conductivity

To our knowledge, data on K_h in elongating grass leaves has not been reported. Spatial distribution of K_h was consistent with the pattern of xylem maturation. At the leaf scale, K_h from the base to 60 mm from the base was almost constant, but rapidly increased 25-fold as the xylem elements matured. The decrease in K_h from 120 mm from the base to the leaf tip reflected the decrease in the number of large bundles and LMX vessel diameter. To emphasize the functional significance of these results, let us consider a typical value for the transpiration of a mature grass leaf, 7 mmol m^{-2} s^{-1} (Zerbi *et al.*, 1991). Using the Poiseuille equation and our data on axial conductivity, the corresponding xylem pressure drop from the base of the leaf to the end of the elongation zone would be approx. 0.4 Mpa. This would result in a xylem water potential close to the water potential of the elongating cells (Martre *et al.*, 1999), which would reduce the water flux from the xylem lumen to the growing tissue. However, the rate of transpiration in the growing leaf of tall fescue would certainly be much less than that in the mature leaf, as the growing leaf is still partly rolled, and shaded by the older leaf.

The computation of K_t by individual inner vessel diameter was consistent, as K_t was proportional to K_h. However, K_t predicted by the Poiseuille equation was approx. three times K_h (Fig. 7). Thus, while considering vessels as capillaries of infinite length, we underestimated actual resistance. Considering the occurrence of short vessels (maximum length of 36 mm in a mature leaf of tall fescue, data not shown), it was expected that relevant information on water conductivity could not be derived solely from a cross-sectional view of vessels. In the case of short vessels, as in tall fescue, it is important to take into account the conductivity of the pit membrane and the diameter of the perforation plate. In fern, for example, *c.* 70% of the axial hydraulic resistance was attributable to the pit membrane (Calkin *et al.*, 1986). Moreover, as vessel diameter was elevated to the fourth power, counting a nonfunctional one would have a dramatic effect on K_t computation. Similarly, a systematic error in LMX diameter would result in substantial overestimation of K_t. The Poiseuille equation has been widely used to predict conductivity in the xylem. Results, however, have been variable, with measured conductivity and flows ranging from 20–100% of theoretical values (Dimond, 1966; Calkin *et al.*, 1986; Hargrave *et al.*, 1994).

K_t* and K_h were consistent in the basal part of the leaf up to 80 mm from the base and in the distal part beyond 140 mm. LMX accounted for most of the conductivity 80–140 mm from the base, and probably still contained cytoplasmic and transverse cell wall residue. As shown by Sanderson *et al.* (1988) in barley roots, this residue might reduce conductivity to considerably less than expected on the basis of vessel diameter only. Moreover, in the region where PX overlapped LMX, water had to be transferred via NMX.

Radial hydraulic conductivity and water deposition rate along the elongation zone

The radial water flux associated with cell expansion in the elongation zone is equal to d_{water}. One interesting result of this study was the very close relationship between d_{water} and the sum of protoxylem cell wall perimeters (Fig. 9), which represents the exchange surface area (per unit of vessel length) between the protoxylem and the surrounding mesophyll cells (i.e. between source and sink for the growth-related water flux). Although this correlation could be coincidental, it is consistent with the hypothesis of Canny and coworkers regarding the leaky pipe model, that the radial water transfer rate per unit length of xylem was proportional to the circumference of the vessels (Altus *et al.*, 1985; Canny, 1991). However, Baum *et al.* (2000) found that the difference in d_{water} between control and salt-affected elongating sorghum leaves is best related to the cross-sectional area of PX vessels.

The relationship found here might imply a limitation of water influx to growing cell by the PX cell wall. Nonami *et al.* (1997) showed in growing soybean hypocotyl that the major resistance to water flow lies in the small cell surrounding the PX vessels. The same cell arrangement could be seen in grass leaf cross sections (Esau, 1965), and might account for the close relationship between water deposition rate and the surface area of the PX wall.

Using our data, an estimation of the radial conductivity was made. Assuming the reflection coefficient of the plasmalemma to be equal to one,

the apparent hydraulic conductance of the elongation zone to radial flux at position $\times$ ($Lp_{px}(x)$, per mm^2 of protoxylem cell wall surface area) would be:

$$L_{pr}(x) = \frac{d_{water}(x)}{A(x) \times \Delta\Psi(x)} \qquad \text{Eqn 7}$$

($A(x)$ is the surface exchange area between the PX and mesophyll cells per mm^2 of leaf and $\Delta\Psi$ is the water potential difference between the xylem and the surrounding mesophyll cells (MPa).) In tall fescue leaves elongating in the dark under similar conditions and at the same rate, Martre *et al*. (1999) found a $\Delta\Psi$ of about 0.3 MPa throughout the elongation zone. Combining this value with those for d_{water} (Fig. 2), Lp_{px} was close to 6.5 mmol s^{-1} m^{-2} MPa^{-1}. This is about five times lower than values reported in growing sections of soybean hypocotyls (37 ± 24 mmol m^{-2} s^{-1} MPa^{-1}) by Steudle & Boyer (1984), and about 70 times lower than values reported in midrib tissue of mature maize leaves (494 ± 311 mmol m^{-2} s^{-1} MPa^{-1}) by Westgate & Steudle (1985). Nevertheless, these authors concluded that the method they used probably largely resulted in an overestimation. Moreover, account must be taken of the physical nature of Lp_{px} in growing tissue. Lp_{px} not only reflects the permeability of tissue to water, but also the resistance by yielding walls to the growth-induced water flux (Lockhart, 1965). This could also explain the discrepancy between our own estimation and those published by Steudle & Boyer (1984) and Westgate & Steudle (1985).

In conclusion, although the results of the present study show that there was hydraulic continuity of the xylem throughout the elongating leaf, the pressure drop due to the hydraulic bottleneck in the basal region of the leaf could limit growth when the emerged part of the leaf actively transpired. Further experiments are required to study the implication of the hydraulic architecture of the elongating leaf on the growth process. In particular, the effect of transpiration of fully elongated and elongating leaves on the elongation rate and water status of the xylem and the mesophyll cell in the elongation zone should be analysed.

ACKNOWLEDGEMENTS

This study was supported partly by a grant from the Région Poitou-Charentes to P. Martre. P Martre wishes to acknowledge the contribution of J. P. André (INRA, Antibes), in initiating him in microcasting technique and for critically reading the manuscript and making several useful remarks. We are grateful to Profs J. L. Bonnemain (University of Poitiers, France) and W. K. Silk (UC Davis), and to Drs P. Cruiziat (INRA, Clermont-Ferrand, France), B. Moulia (INRA, Lusignan, France), and P. Fleurat-Lessart (CNRS, Poitiers, France) for offering invaluable suggestions and stimulating discussion during the course of this work. We are also indebted to K. Lynch (INRA translation unit, Jouy-en-Josas, France) for revising the English version of the manuscript. We thank Ms L. Cousson, Mrs G. Millet and P. Poussot for their skilled technical assistance.

REFERENCES

Altus DP, Canny MJ, Blackman DR. 1985. Water pathways in wheat leaves. II. Water-conducting capacities and vessel diameters of different vein types, and the behaviour of the integrated vein network. *Australian Journal of Plant Physiology* **12**: 183–199.

André JP. 1993. Microcasting of intra- and inter cellular spaces in plant tissues. *Comptes Rendus de l'Académie des Sciences de Paris, Sciences de la Vie* **316**: 1336–1341.

Barlow EWR. 1986. Water relations of expanding leaves. *Australian Journal of Plant Physiology* **13**: 45–58.

Baum SF, Silk WK, Tran TN. 2000. Effects of salinity on xylem structure and water use in growing leaves of *Sorghum*. *New Phytologist* **145**:000–000. .

Bierhorst DW, Zamora PM. 1965. Primary xylem elements and element associations of angiosperms. *American Journal of Botany* **52**: 657–710.

Calkin HW, Gibson AC, Nobel PS. 1986. Biophysical model of xylem conductance in tracheids of the fern Ptersi vittata. *Journal of Experimental Botany* **37**: 1054–4064.

Canny MJ. 1991. The xylem wedge as a functional unit-speculations on the consequences of flow in leaky tubes. *New Phytologist* **118**: 367–374.

Dale JE. 1985. The carbon relations of the developing leaf. In: Baker NR, Davies WJ, Ong CK, eds. *Control of leaf growth*. Cambridge, UK: Cambridge University Press, 135–154.

Dimond AE. 1966. Pressure and flow relations in vascular bundles of the tomato plant. *Plant Physiology* **441**: 119–131.

Dong Z, McCully ME, Canny MJ. 1997. Does *Acetobacter diazotrophicus* live and move in the xylem of sugarcane stems? Anatomical and physiological data *Annals of Botany* **80**: 147–158.

Durand JL, Onillon B, Schnyder H, Rademacher I. 1995. Drought effects on cellular and spatial parameters of leaf growth in tall fescue. *Journal of Experimental Botany* **46**: 1147–1155.

Durand JL, Schäufele R, Gastal F. 1999. Grass leaf elongation rate as a function of developmental stage and temperature: Morphological analysis and modelling. *Annals of Botany* **83**: 577–588.

Ellis RP. 1976. A procedure for standardizing comparative leaf anatomy in the *Poaceae*. I. The leaf-blade as viewed in transverse section. *Bothalia* **12**: 65–109.

Esau K. 1953. Primary vascular differentiation in plants. *Biological Review* **29**: 46–86.

Esau K. 1965. *Plant anatomy. 2nd edn*, New York, USA: John Wiley & Sons.

Evert RF, Botha CEJ, Mierzwa RJ. 1985. Free-space marker studies on the leaf of *Zea mays* L. *Protoplasma* **126**: 62–73.

Evert RF, Russin WA, Bosabalidis AM. 1996. Anatomical and ultrastructural changes associated with sink-to-source transition in developing maize leaves. *International Journal of Plant Sciences* **157**: 247–261.

Frensch J. 1997. Primary responses of root and leaf elongation to water deficits in the atmosphere and soil solution. *Journal of Experimental Botany* **48**: 985–999.

Fricke W, Flowers TJ. 1998. Control of leaf cell elongation in barley. Generation rates of osmotic pressure and turgor, and growth-associated water potential gradients. *Planta* **206**: 53–65.

Fukazawa K, Imagawa H. 1981. Quantitative analysis of lignin using an UV microscopic image analyser. Variation within one growth increment. *Wood Science and Technology* **15**: 45–55.

Goodwin RH. 1942. On the development of xylary elements in the first internode of avena in dark and light. *American Journal of Botany* **29**: 818–828.

Hargrave KR, Kolb KJ, Ewers FW, Davis SD. 1994. Conduit diameter and drought-induced embolism in *Salvia mellifera* greene. *New Phytologist* **126**: 695–705.

Lewis AM, Boose ER. 1995. Estimating volume flow rates through xylem conduits. *American Journal of Botany* **82**: 1112–1116.

Lockhart JA. 1965. An analysis of irreversible plant cell elongation. *Journal of Theoretical Biology* **8**: 264–276.

MacAdam JCW. 1988. *Cellular dynamics, peroxidase activity, and secondary cell wall deposition during tall fescue leaf blade development*. PhD thesis, University of Missouri, Columbia MO, USA.

Martre P, Bogeat-Triboulot MB, Durand JL. 1999. Measurement of a growth-induced water potential gradient in tall fescue leaves. *New Phytologist* **142**: 435–439.

Matsuda K, Riazi A. 1981. Stress-induced osmotic adjustment in growing regions of barley leaves. *Plant Physiology* **68**: 571–576.

Maurice I, Gastal F, Durand JL. 1997. Generation of form and associated mass deposition during leaf development in grasses: a kinematics approach for non-steady growth. *Annals of Botany* **80**: 673–683.

Michelena VA, Boyer JS. 1982. Complete turgor maintenance at low water potentials in the elongating region of maize leaves. *Plant Physiology* **69**: 1145–1149.

Nonami H, Wu Y, Boyer JS. 1997. Decreased growth-induced water potential. A primary cause of growth inhibition at low water potentials. *Plant Physiology* **114**: 501–509.

O'Brien TP. 1981. The primary xylem. In: Barnett JR, ed. *Xylem cell development*. Turnbridge Wells, UK: Castle House Publication Ltd, 14–46.

Paolillo DJ. 1995. Protoxylem maturation in the seedling of wheat. *American Journal of Botany* **82**: 337–355.

Paolillo DJ, Rubin G. 1991. Relative elemental rates of elongation and the protoxylem-metaxylem transition in hypocotyls of soybean seedlings. *American Journal of Botany* **78**: 845–854.

Rayan A, Matsuda K. 1988. The relation of the anatomy to water movement and cellular response in young barley leaves. *Plant Physiology* **87**: 853–858.

Ryser U, Schorderet M, Zhao GF, Studer D, Ruel K, Hauf G, Keller B. 1997. Structural cell-wall proteins in protoxylem development: evidence for a repair process mediated by glycine-rich protein. *The Plant Journal* **12**: 97–111.

Sanderson J, Whitbread FC, Clarkson DT. 1988. Persistent xylem cross-walls reduce the axial hydraulic conductivity in the apical 20 cm of barley seminal root axes: implications for the driving force for water movement. *Plant, Cell & Environment* **11**: 247–256.

Savidge RA. 1996. Xylogenesis, genetic and environmental regulation. A review. *International Association of Wood Anatomists Bulletin* **17**: 269–310.

Schnyder H, Nelson CJ. 1987. Growth rates and carbohydrate fluxes within the elongation zone of tall fescue leaf blades. *Plant Physiology* **85**: 548–553.

Schnyder H, Nelson CJ. 1988. Diurnal growth of tall fescue leaf blades. I. spatial distribution of growth, deposition of water, and assimilate import in the elongation zone. *Plant Physiology* **86**: 1070–1076.

Schnyder H, Nelson CJ, Coutts H. 1987. Assessment of spatial distribution of growth in the elongation zone of grass leaf blades. *Plant Physiology* **85**: 290–293.

Sharman BC. 1942. Developmental anatomy of the shoot of *Zea mays* L. *Annals of Botany* **6**: 245–282.

Silk WK. 1984. Quantitative descriptions of development. *Annual Review of Plant Physiology* **35**: 479–518.

Sperry JS, Donnelly JR, Tyree MT. 1988. A method for measuring hydraulic conductivity and embolism in xylem. *Plant, Cell & Environment* **11**: 35–40.

St Aubin G, Canny MJ, McCully ME. 1986. Living vessel elements in the late metaxylem of sheathed maize roots. *Annals of Botany* **58**: 577–588.

Steudle E, Boyer JS. 1984. Hydraulic resistance to radial water flow in growing hypocotyl of soybean measured by a pressure-perfusion technique. *Planta* **164**: 189–200.

Trivett CL, Evert RF. 1998. Ontogeny of the vascular bundles and contiguous tissues in the barley leaf blade. *International Journal of Plant Sciences* **159**: 716–723.

Westgate ME, Boyer JS. 1984. Transpiration- and growth-induced water potentials in maize. *Plant Physiology* **74**: 882–889.

Westgate ME, Steudle E. 1985. Water transport in the midrib tissue of maize leaves. Direct measurement of the propagation of changes in cell turgor across a plant tissue. *Plant Physiology* **78**: 183–191.

Zerbi G, Morgan JA, Lecain DR. 1991. Gas exchange and water relations in water and salinity stressed wheat lines. *Journal of Agronomy and Crop Science* **166**: 1–7.